

# Empirical Modelling of ReRAM Measured Characteristics Using Charge and Flux

M. M. Al Chawa<sup>\*</sup>, C. de Benito<sup>†‡</sup>, H. Castan<sup>§</sup>, S. Dueñas<sup>§</sup>, S. G. Stavrinos<sup>¶</sup>, R. Tetzlaff<sup>\*</sup>, and R. Picos<sup>†‡</sup>

<sup>\*</sup> Institute of Circuits and Systems, Technische Universität Dresden, Dresden, Germany

<sup>†</sup> Industrial Engineering and Construction Dept., Universitat de les Illes Balears, Palma, Mallorca, Spain

<sup>‡</sup> Balearic Islands Health Institute (IdISBa) Palma, Mallorca, Spain

<sup>§</sup> Department of Electronics, University of Valladolid, Valladolid, Spain

<sup>¶</sup> School of Science and Technology, International Hellenic University, Thessaloniki, Greece

**Abstract**—In this work, an empirical model based on a pure relation between charge and flux (aka an ideal memristor) has been proposed to fit the experimental data for ReRAM devices in flux charge domain. The model is able to capture the behavior with a very good accuracy, including also the behavior of the memconductance.

**Index Terms**—ReRAM; memristor; modeling; flux; charge.

## I. INTRODUCTION

Until Leon Chua proposed it during the early 70s [1], nobody had noticed the possible symmetry between the current  $i$ , the voltage  $v$ , the charge  $q$  and the flux  $\varphi$  in electric theory. There were three elements relating charge and voltage (the capacitor), flux and current (inductor), and current and voltage (resistor). However, the relation between charge and flux was missing, so Chua proposed the existence of a new fourth electrical element. This new element would behave as a resistor with a memory, and thus the name 'memristor'.

Actually, these elements had been already described long time ago [2], though they had never been used in circuit theory. In addition, Chua's work paved the way to the generalization of a class of devices and systems (memristive systems or devices) which are intrinsically nonlinear and can be described by a set of differential equations relating the electrical magnitudes to an internal state variable [3].

Currently, these novel devices are considered as one of the most promising elements for the next generation of integrated circuit (IC), beyond and more than Moore [4]. As an example of application, they may provide a way to escape the classical bottleneck problem created by the need to move data between memory and the processor. Some of the areas where this is forecast to be beneficial are the Internet-of-Things (IoT) and other edge computing applications. This way, many different applications using memristor-based architectures are being proposed: new memory devices (ReRAMs, MRAM, etc.) [5]–[7], innovative devices for sensing applications [8], [9], or building blocks for bio-inspired systems (artificial neural networks (ANNs) and other) [10], among others.

## II. FLUX-CHARGE SPACE DESCRIPTION OF MEMRISTIVE DEVICES

The election of the electrical variables to describe a device is not usually a problem. The common variables are current and voltage. However, some advantages may be obtained by using the flux and charge, as proposed in the literature [11]–[17]). This description can provide a simpler set of differential equations than using the  $V - I$  pair.

A memristive device is described as a two terminal element [12], with a voltage difference between the terminals named  $V(t)$ , and a current  $I(t)$  passing through it. The alternate description uses the flux  $\phi(t)$  (also called voltage first momentum) instead of voltage, and the charge  $Q(t)$  (or current first momentum) instead of the current. The relation between these variables is defined by:

$$\phi(t) = \int_{-\infty}^t V(\tau) d\tau \quad (1)$$

and

$$Q(t) = \int_{-\infty}^t I(\tau) d\tau \quad (2)$$

More details about the *flux* and *charge* in the previous equations can be found in [12]. In the current context, these terms are defined by the integrals defined above. The original definition of an *ideal* memristor controlled by flux is provided by a nonlinear relation:

$$Q = f(\phi, V) \quad (3)$$

Later on, this description in (3) was improved by including state variables, that included additional behaviors.

The new memristor device class was named *extended* memristors. This extended memristor defines a new internal state vector  $\mathbf{X}$ , of dimension  $k$ , that includes all the internal states of the device.

$$\mathbf{X} = (x_1, x_2, \dots, x_k) \quad (4)$$

where the dynamics of these state variables can be defined as follows

$$\frac{d\mathbf{X}}{dt} = \mathbf{g}(\phi, V, \mathbf{X}) \quad (5)$$

This set of equations can be regarded as the description of a surface in an N-dimensional phase space. This description has been shown to be useful for a semi-empirical description of the behavior of memristive devices [18], [19].

Using the charge and flux description, an extended memristor may be described as follows

$$Q = f(\phi, V, \mathbf{X}) \quad (6)$$

As a case of interest, it was proposed that memristive RAMs (ReRAMs) are actually a kind of memristors [13]. In this case, one could use the variables describing the geometry of a CF (conductive filament) or the size of the gap between the CF and electrode, as well as the filament temperature [20]–[25].

### III. EXPERIMENTAL SETUP AND MEASUREMENTS

The study was carried out using  $TiN/Ti/HfO_2/W$  metal–insulator–metal (MIM) capacitors as resistive switching devices [26]. The first step of the fabrication process was the deposition of a 20 nm-thick Ti adherence layer on a 100 mm-diameter Si-n++ wafer, followed by the deposition of a 50 nm-thick W layer. Magnetron sputtering was used to grow both of those layers. Next, a plasma-enhanced chemical vapor deposition (PECVD) using silane (SiH<sub>4</sub>) as the precursor process was used to create a 100 nm SiO<sub>2</sub> isolation oxide, which was patterned using photolithography and dry etching.

The apertures of the SiO<sub>2</sub> layer define the active area of the MIM devices. After that, the 10 nm HfO<sub>2</sub> film was deposited by atomic layer deposition (ALD) at 225 °C using Tetrakis(dimethylamino)hafnium (TDMAH) and H<sub>2</sub>O as precursors and N<sub>2</sub> as the carrier and purge gas. Magnetron sputtering was used to create the top electrode, obtaining a metal layer of 10 nm-thick Ti and a 200 nm-thick TiN. The electrode was patterned by a lift-off process.

As the last step, a 500 nm Al layer was deposited on the back of the wafer by magnetron sputtering for electrically contacting the Wbottom electrode through the Si-n++ substrate used to fabricate the devices. The final TiN/Ti/HfO<sub>2</sub>/W devices present a square shape, and the fabricated areas range between 2×2 m<sup>2</sup> and 120×120 m<sup>2</sup>.

The signal used to drive the device is shown in Fig. 1. It is a triangular current waveform, with a raising amplitude. The resulting IV characteristics are depicted in Fig. 2

### IV. MODEL DESCRIPTION

As has been said above, the main trend for memristor modeling is using the  $V - I$  variable pair. In the presented case, we have instead decided to check the possibility of using  $\phi - Q$ . This modeling approach has been proposed to simplify the model description, being closer to the original conception of the electrical element [1], [27], [28].

In this work we have considered an ideal memristor for simplicity. This simplification of the model dose not affect the fitting accuracy. A nonlinear relation of the  $\phi - Q$  variable pair

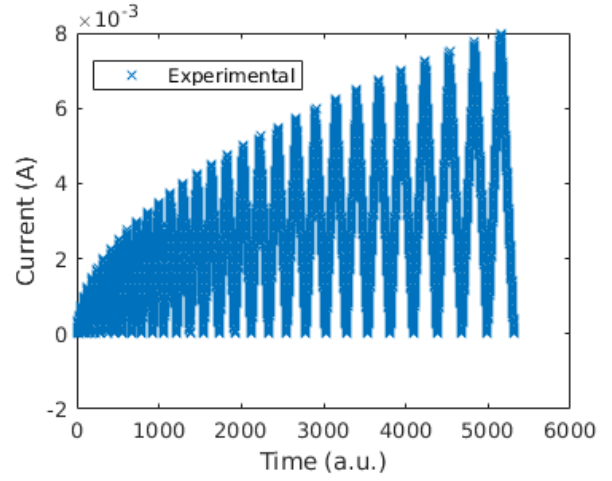


Fig. 1. Current signal applied to the system under test.

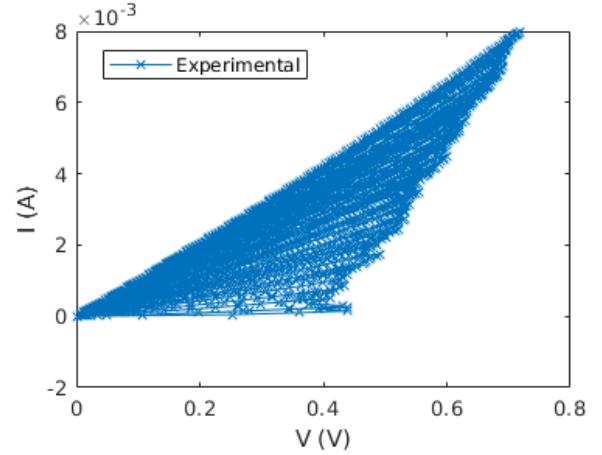


Fig. 2. Measured IV characteristics of the ReRAM device.

[14], [21], [29] is proposed for describing ReRAM memristive devices as:

$$Q = Q_0 \cdot \left( \frac{\phi}{\phi_0} \right)^{1+n} \quad (7)$$

From the definition of charge and flux, the current can be found by taking the derivative of the charge as follows:

$$I = \frac{dQ}{dt} \quad (8)$$

and the conductance is found to be

$$G = \frac{dQ}{d\phi} \quad (9)$$

It is worth to point out that  $n$  is a parameter depending on all the state variables  $\mathbf{X}$ , in addition to the flux and input voltage signal. In this work, we have further simplified the model by considering the device to be an ideal memristor controlled by flux (i.e.  $n \approx \text{constant}$  and  $\frac{dn}{dt} \approx 0$ ) [30].

The variables of interest ( $\phi$  and  $Q$ ) are defined by the relations in (1) and (2), respectively, as suggested in [12].

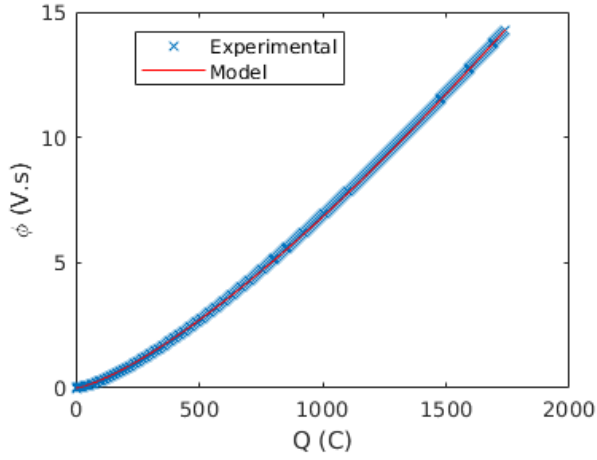


Fig. 3. Experimental (blue) and modelled (red) charge vs flux.

Numerical integration of the input voltage signal and the measured current can be used to calculate the flux and charge, where  $Q_0$  and  $\phi_0$  are fitting parameters, which can be calculated as the maximum values of the experimental data, and  $n$  is obtained by fitting the logarithmic slope of the charge vs the flux. Under these assumptions, (7), and (9) determine the dynamic behaviour of the measured ReRAM memristive device.

## V. RESULTS

We have fitted the parameters in equation 7 to the experimental data using a two-step process: first, we have obtained the experimental charge ( $Q_e$ ) and flux ( $\phi_e$ ) by performing a numerical integration of the measured IV data. As a second step, we have fitted Eq. 7 to these  $Q_e$  and  $\phi_e$ . The values of the fitted parameter are  $Q_0 = 14.3C$ ,  $\phi_0 = 1741V.s$ , and  $n = 1/3$ . The quality of the fitting can be observed in Fig. 3. Notice that the experimental charge and flux shown in the figure correspond to the numerical integration of all the cycles in Fig. 2.

Once the model has its parameters defined, we can obtain other electrical magnitudes directly by derivation. The obtained IV characteristics from the model are shown in Fig. 4, providing a very close fit. The evolution of the current versus time as obtained from the model is depicted in Fig. 5 and, finally, the evolution of the conductance versus time is illustrated in Fig. 6.

It has to be noted that there is a ripple in this last figure, which may be attributed to the presence of a parasitic capacitor, that has not been considered in the model.

## VI. CONCLUSION

As has been shown in the paper, the considered ReRAM devices can be modelled as ideal memristors using the formal framework proposed by Corinto et al [12]. In this work, we have shown that a very simple model relating charge and flux with a nonlinear relation provides a very good fitting of the

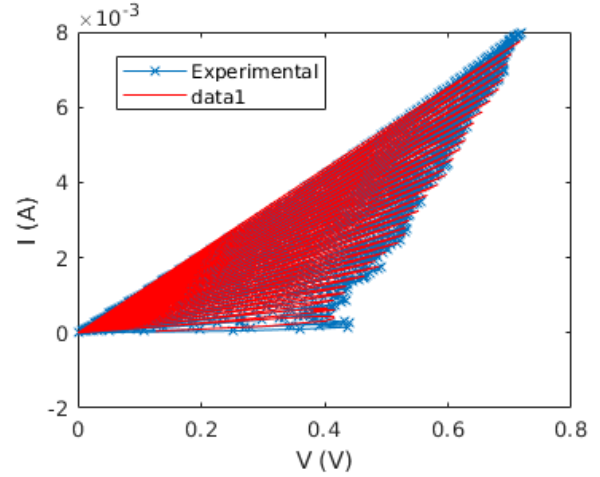


Fig. 4. Experimental (blue) and modelled (red) IV characteristics.

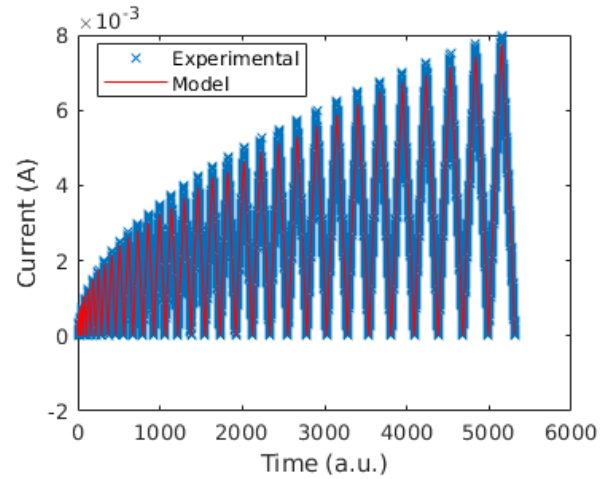


Fig. 5. Experimental (blue) and modelled (red) current vs time.

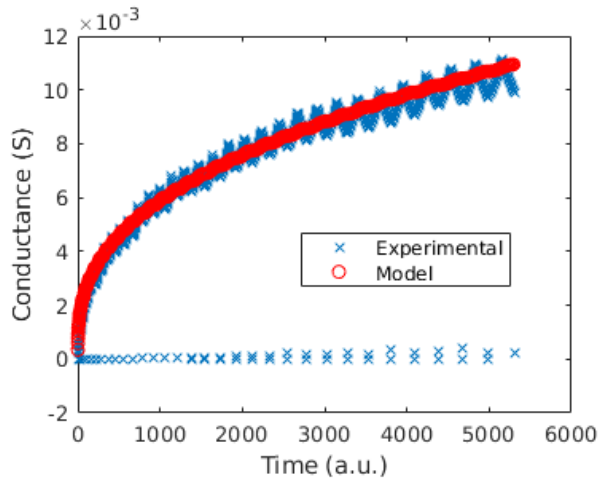


Fig. 6. Experimental (blue) and modelled (red) conductance.

experimental results. Thus, since no other variables need to be considered, the device can be used as an ideal memristor.

Further work related to this should be performed to check this conclusion. Specifically, the effect of the input signal velocity has to be tested, as well as the variability in the cycle to cycle switching characteristics.

## REFERENCES

- [1] L. Chua, "Memristor-the missing circuit element," *IEEE Transactions on circuit theory*, vol. 18, no. 5, pp. 507–519, 1971.
- [2] T. Prodromakis, C. Toumazou, and L. Chua, "Two centuries of memristors," *Nature materials*, vol. 11, no. 6, pp. 478–481, 2012.
- [3] L. Chua and S. M. Kang, "Memristive devices and systems," *Proceedings of the IEEE*, vol. 64, no. 2, pp. 209–223, Feb 1976.
- [4] R. Tetzlaff, *Memristors and memristive systems*. Springer, 2013.
- [5] H. Kim, M. P. Sah, C. Yang, and L. O. Chua, "Memristor-based multilevel memory," in *Cellular nanoscale networks and their applications (CNNA), 2010 12th international workshop on*. IEEE, 2010, pp. 1–6.
- [6] S. Stathopoulos, A. Khiat, M. Trapatseli, S. Cortese, A. Serb, I. Valov, and T. Prodromakis, "Multibit memory operation of metal-oxide bi-layer memristors," *Scientific reports*, vol. 7, no. 1, pp. 1–7, 2017.
- [7] K. Eshraghian, K.-R. Cho, O. Kavehei, S.-K. Kang, D. Abbott, and S.-M. S. Kang, "Memristor mos content addressable memory (mcam): Hybrid architecture for future high performance search engines," *IEEE Transactions on Very Large Scale Integration (VLSI) Systems*, vol. 19, no. 8, pp. 1407–1417, 2011.
- [8] S. Carrara, D. Sacchetto, M.-A. Doucey, C. Baj-Rossi, G. De Micheli, and Y. Leblebici, "Memristive-biosensors: A new detection method by using nanofabricated memristors," *Sensors and Actuators B: Chemical*, vol. 171, pp. 449–457, 2012.
- [9] I. Gupta, A. Serb, A. Khiat, R. Zeitler, S. Vassanelli, and T. Prodromakis, "Memristive integrative sensors for neuronal activity," *arXiv preprint arXiv:1507.06832*, 2015.
- [10] Y. V. Pershin and M. Di Ventra, "Experimental demonstration of associative memory with memristive neural networks," *Neural Networks*, vol. 23, no. 7, pp. 881–886, 2010.
- [11] Y. Xie, "Emerging memory technologies," 2014.
- [12] F. Corinto, P. P. Civalleri, and L. O. Chua, "A theoretical approach to memristor devices," *IEEE Journal on Emerging and Selected Topics in Circuits and Systems*, vol. 5, no. 2, pp. 123–132, 2015.
- [13] L. Chua, "Resistance switching memories are memristors," *Applied Physics A*, vol. 102, no. 4, pp. 765–783, 2011.
- [14] R. Picos, J. B. Roldan, M. M. Al Chawa, P. Garcia-Fernandez, F. Jimenez-Molinos, and E. Garcia-Moreno, "Semiempirical modeling of reset transitions in unipolar resistive-switching based memristors," *RADIOENGINEERING*, vol. 24, no. 2, p. 421, 2015.
- [15] S. Shin, K. Kim, and S.-M. Kang, "Compact models for memristors based on charge-flux constitutive relationships," *Computer-Aided Design of Integrated Circuits and Systems, IEEE Transactions on*, vol. 29, no. 4, pp. 590–598, 2010.
- [16] M. M. Al Chawa, R. Picos, E. Garcia-Moreno, S. Stavriniades, J. Roldan, and F. Jimenez-Molinos, "An analytical energy model for the reset transition in unipolar resistive-switching rams," in *Electrotechnical Conference (MELECON), 2016 18th Mediterranean*. IEEE, 2016, pp. 1–4.
- [17] R. Picos, M. M. Al Chawa, M. Roca, and E. Garcia-Moreno, "A charge-dependent mobility memristor model," in *Proceedings of the 10th Spanish Conference on Electron Devices, CDE'2015*. IEEE, 2015.
- [18] D. Maldonado, M. B. Gonzalez, F. Campabadal, F. Jimenez-Molinos, M. M. Al Chawa, S. G. Stavriniades, J. B. Roldan, R. Tetzlaff, R. Picos, and L. O. Chua, "Experimental evaluation of the dynamic route map in the reset transition of memristive rams," *Chaos, Solitons & Fractals*, vol. 139, p. 110288, 2020.
- [19] R. Picos, M. M. Al Chawa, C. de Benito, S. G. Stavriniades, and L. O. Chua, "Using self-heating resistors as a case study for memristor compact modelling," *IEEE Journal of the Electron Devices Society*, 2022.
- [20] D. Ielmini, "Resistive switching memories based on metal oxides: mechanisms, reliability and scaling," *Semiconductor Science and Technology*, vol. 31, no. 6, p. 063002, 2016.
- [21] M. M. Al Chawa, R. Picos, J. B. Roldan, F. Jimenez-Molinos, M. A. Villena, and C. de Benito, "Exploring resistive switching-based memristors in the charge-flux domain: a modeling approach," *International Journal of Circuit Theory and Applications*, vol. 46, no. 1, pp. 29–38, 2018, cta.2397. [Online]. Available: <http://dx.doi.org/10.1002/cta.2397>
- [22] R. Picos, J. Roldan, M. M. Al Chawa, F. Jimenez-Molinos, and E. Garcia-Moreno, "A physically based circuit model to account for variability in memristors with resistive switching operation," in *Design of Circuits and Integrated Systems (DCIS), 2016 Conference on*. IEEE, 2016, pp. 1–6.
- [23] S. Kim, Y. Chang, M. Kim, S. Bang, T. Kim, Y. Chen, J. Lee, and B. Park, "Ultralow power switching in a silicon-rich sily/sinx double-layer resistive memory device," *Physical chemistry chemical physics: PCCP*, vol. 19, no. 29, p. 18988, 2017.
- [24] C.-Y. Lin, P.-H. Chen, T.-C. Chang, K.-C. Chang, S.-D. Zhang, T.-M. Tsai, C.-H. Pan, M.-C. Chen, Y.-T. Su, Y.-T. Tseng *et al.*, "Attaining resistive switching characteristics and selector properties by varying forming polarities in a single hfo2-based rram device with a vanadium electrode," *Nanoscale*, vol. 9, no. 25, pp. 8586–8590, 2017.
- [25] J. B. Roldán, G. González-Cordero, R. Picos, E. Miranda, F. Palumbo, F. Jiménez-Molinos, E. Moreno, D. Maldonado, S. B. Baldomá, M. Moner Al Chawa *et al.*, "On the thermal models for resistive random access memory circuit simulation," *Nanomaterials*, vol. 11, no. 5, p. 1261, 2021.
- [26] S. Poblador, M. Maestro-Izquierdo, M. Zabala, M. B. Gonzalez, and F. Campabadal, "Methodology for the characterization and observation of filamentary spots in hfox-based memristor devices," *Microelectronic Engineering*, vol. 223, p. 111232, 2020.
- [27] M. M. Al Chawa, C. de Benito, and R. Picos, "A simple piecewise model of reset/set transitions in bipolar rram memristive devices," *IEEE Transactions on Circuits and Systems I: Regular Papers*, vol. 65, no. 10, pp. 3469–3480, 2018.
- [28] M. M. Al Chawa, R. Picos, and R. Tetzlaff, "A simple memristor model for neuromorphic rram devices," in *2020 IEEE International Symposium on Circuits and Systems (ISCAS), 2020*, pp. 1–1.
- [29] M. M. Al Chawa and R. Picos, "A simple quasi-static compact model of bipolar rram memristive devices," *IEEE Transactions on Circuits and Systems II: Express Briefs*, 2019.
- [30] M. M. A. Chawa, R. Picos, and R. Tetzlaff, "A compact memristor model for neuromorphic rram devices in flux-charge space," *IEEE Transactions on Circuits and Systems I: Regular Papers*, vol. 68, no. 9, pp. 3631–3641, 2021.